Nanoscale

MINIREVIEW

View Article Online
View Journal | View Issue

Cite this: *Nanoscale*, 2019, **11**, 14993

Graphitic carbon nitride-based nanocomposites and their biological applications: a review

Ming-Hsien Chan,[a] Ru-Shi Liu *[a,b,c] and Michael Hsiao *[a,d]

Received 29th May 2019,
Accepted 9th July 2019

DOI: 10.1039/c9nr04568f

rsc.li/nanoscale

Quantum dots (QDs) have extensive application prospects in the fields of optics, magnetism, catalysis, and biomedicine. New carbon-doped QDs are currently being used in these research fields. Graphitic carbon nitride QDs (g-CNs) composed of only carbon and nitrogen have attracted attention because of their unique optical and catalytic properties. g-CNs have numerous electronic properties and can be used as photocatalytic modifiers in a wide range of applications in electrochemistry. Additionally, g-CNs also have biological potential and due to their chemical composition have extremely low toxicity; their blue light emission can be applied to biological imaging, and their appropriate energy level (2.7 eV) allows electrons to be deposited on their surface, which allows g-CNs to be used as photosensitizers in optical therapy. Finally, g-CNs can be combined with other nanomaterials to form composite materials, which can result in new advantages not seen in either of the materials alone. In this manuscript, we thoroughly report the most recent findings regarding the synthesis of g-CNs and their respective properties. We report the advantages of g-CNs conferred by their unique properties and their advantages for application in current biology and medicines.

1. Introduction

Quantum dots (QDs), also known as semiconductor nanocrystals, have extensive application prospects in the fields of optics, magnetism, and catalysis as well as biological applications. However, such materials decompose easily at high concentrations or under light irradiation, which leads to the release of deadly heavy metal ions, posing a potential threat to organisms and the environment. Therefore, finding nontoxic nanomaterials with similar optical properties has become a

[a]*Genomics Research Center, Academia Sinica, Taipei 115, Taiwan. E-mail: rsliu@ntu.edu.tw, mhsiao@gate.sinica.edu.tw*
[b]*Department of Chemistry, National Taiwan University, Taipei 106, Taiwan*
[c]*Department of Mechanical Engineering and Graduate Institute of Manufacturing Technology, National Taipei University of Technology, Taipei 106, Taiwan*
[d]*Department of Biochemistry, College of Medicine, Kaohsiung Medical University, Kaohsiung 807, Taiwan*

Ming-Hsien Chan

Ming-Hsien Chan received his Bachelor and Master's degree in the department of bioscience and biotechnology from National Taiwan Ocean University in 2014. He obtained a Ph.D. degree in chemistry from National Taiwan University in 2018. Now, he is a postdoctoral fellow in Prof. Hsiao's group at Genomics Research Center, Academia Sinica. His current research interests include the synthesis of biological nanomaterials and their application in vitro *and* in vivo.

Ru-Shi Liu

Ru-Shi Liu is currently a professor at the Department of Chemistry, National Taiwan University. He received his Bachelor's degree in Chemistry from Shoochow University (Taiwan) in 1981. He received his Master's degree in nuclear science from the National TsingHua University (Taiwan) in 1983. He obtained two Ph.D. degrees in chemistry – one from National TsingHua University in 1990 and one from the University of Cambridge in 1992. His research concerns the field of materials chemistry.

key focus of research. Carbon is one of the most abundant elements on the Earth, and its new form, graphitic carbon nitride QDs (g-CNs, or named g-C_3N_4), emits stable fluorescence, and also has a wide excitation wavelength range, both of which allow g-CNs to be used as biomarkers in living organisms.[1] Moreover, after surface modification or doping, the fluorescence emission quantum yield of g-CNs is comparable to that of high-performance semiconductor QDs. These QDs, however, are safer than other fluorescent materials, are more fluorescent than other fluorescent markers, and do not significantly interfere with the activity of biomolecules. The advantages of g-CNs to other nanomaterials are also reflected in that the parameters of the functional groups on their surface can be adjusted to control their photoelectric properties, solubility, and compatibility with various interfaces.[2] Tri-*s*-triazine structure-based g-CNs are a polymeric material consisting of C, N, and a small amount of H impurity.[3] In various carbon-based materials, the surface of g-CNs has electron-rich properties and multiple surface-modified functionalities.[4] Currently, the application of g-CNs is not yet clear, which means that g-CNs have not been studied well. Initially, g-CNs were primarily used as solid lubricants. Until 2008, g-CNs were used as photocatalysts.[5] Their advantage is that they are metal-free and can be used for photocatalytic water decomposition, so g-CNs are new photocatalysts. Research related to water decomposition *via* g-CNs represents a milestone in g-CN research regarding their photocatalytic applications. The most important property of g-CNs is that these novel materials do not contain metal elements, which is appealing because most current photocatalysts contain metals, and these metallic elements can cause environmental toxicity and lead to unnecessary damage. Because g-CNs are metal free, they can be applied in biological research. The fact that g-CNs are composed of pure carbon and nitrogen compounds is undoubtedly favorable in regard to their biocompatibility. In the current study, thermal stripping or hydrothermal methods can be used to obtain g-CN QDs that can be applied in fluorescent probes as cell markers to enter into cells for cell tracking and imaging.[6] This use of g-CNs highlights that they can be used in important research, such as tumor cell imaging.[7] There are, however, some difficulties regarding the optical positioning of g-CNs. The absorption and excitation wavelengths of g-CNs are located in the UV-Vis region, making it difficult for the fluorescence of g-CNs to penetrate the skin layer and may be potentially harmful to the human body. These drawbacks are problems in biological applications of g-CNs. First, we discuss the physical and chemical properties of raw synthetic g-CNs in the following section.

Second, we use these properties as a starting point to discuss the applications of g-CN technology. Third, we propose how the nanocomposite materials of current g-CNs can be effectively applied in the field of biomedicine. Finally, the current applications of g-CNs will be integrated to discuss their potential in future research.

2. Basis of graphitic carbon nitride quantum dots

This section introduces the basic concepts of g-CNs. First, we discuss basic QDs composed of carbon. Second, we introduce the method of synthesizing g-CNs. Finally, we discuss the characteristics of g-CNs to describe their potential for future applications, which is the most important part of this study. A discussion of how g-CNs became a popular research topic as well as another nanomaterial is also presented. Finally, the current problems that must be overcome in the application of g-CNs are described.

2.1 The history of g-CN discovery

Research into this topic started when A. Y. Liu and M. L. Cohen replaced C with Si in the crystal structure of β-Si_3N_4 in 1989. They attempted to use the local density states and the first pseudopotential approximation method to theoretically predict β-C_3N_4 (*i.e.*, carbon nitride). β-C_3N_4, which has a hardness comparable to that of diamond, is a novel compound and is not found in nature. In 1996, Teter and Hemley, using calculation methods, determined that g-CNs have five structural types: α-phase, β-phase, a cubic phase, quasi-cubic phase, and graphitic-like phase. With the exception of the graphitic-like phase, the hardness of the other four material types is comparable to that of diamond. Although the graphite phase does not have high hardness, its unique electronic structure and excellent chemical stability make it highly valued (Fig. 1a).[8] The suitable band gap (2.7 eV) of g-CNs means that they can emit visible light (approximately 400 to 475 nm). Luminescent g-CNs have unique optical properties, such as a stable fluorescence signal, no light scintillation, and adjustable emission wavelength (Fig. 1b). In addition to their optical advantages, g-CNs have low biotoxicity and good biocompatibility and have gradually become a research hotspot among carbon nanomaterials. This section also explores the reaction mechanism of g-CN fluorescence and describes the advances of g-CNs in biomedical applications (Fig. 2a).

Michael Hsiao

Michael Hsiao is currently a research fellow at the Genomics Research Center, Academia Sinica. He received his D.V.M. degree from National Taiwan University in 1983. He obtained a Ph.D. degree in pathology from the University of Southern California in 1991. His research concerns the field of targeting tumor growth/survival pathways to enhance tumor chemosensitivity and/or radiosensitivity, the novel strategies to overcome tumor metastasis, and the development of nanoparticle-mediated high-throughput transfection platforms.

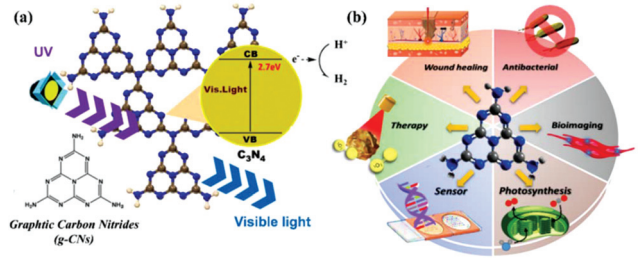

Fig. 1 Basic composition and biological applications of g-CNs. (a) g-CNs are tri-*s*-triazine structured nanomaterials in a 2D plane. g-CNs have the appropriate energy level to absorb UV light and produce blue light. Free electrons can convert H^+ to H_2 or O_2 to O_2^-. The high activity of the surface of g-CNs makes their application surface very diverse. (b) g-CNs have many biological applications, such as antibacterial applications due to their ability to produce reactive oxygen species, biological fluorescence imaging applications due to their visible light fluorescence, chloroplast applications which can be attributed to their presence of free electrons that promote light synthesis, biosensing applications because g-CNs with a 2D structure can be used as biological nanosubstrates, cancer treatment applications because the oxidative pressure generated by the absorption of light energy can kill cancer cells, and antibacterial applications because their antibacterial properties can improve the efficiency of wound healing.

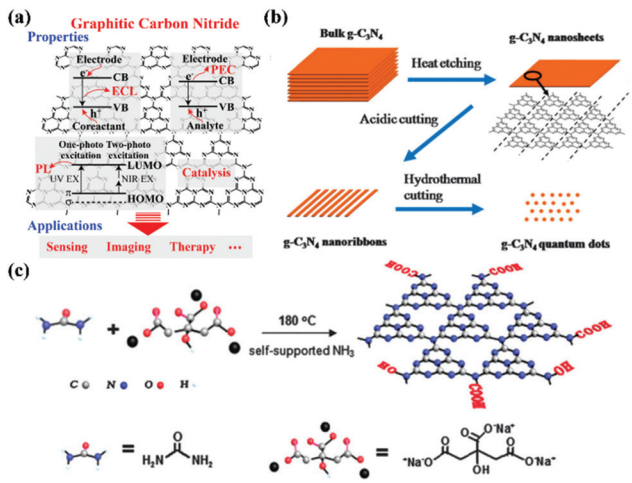

Fig. 2 Electronic configuration and synthesis of g-CNs. (a) g-CNs have a variety of electron transfer methods that release energy in an electrochemiluminescence (ECL), persistent luminescence (PL), and photoelectrochemical (PEC) after absorbing light energy. This electrochemical activity allows g-CNs to be used in biosensing, bioimaging, and therapeutic applications. Reproduced with permission.[6] Copyright 2016, Wiley Online Library. (b) Currently, the main method of synthesizing g-CNs is "top-down". The thermal etching split method can lead to the controllable synthesis of g-CN nanosheets, nanoribbons and quantum dots. (c) Another synthesis method is the "bottom-up" method for a small molecular composition, mainly using C and N-containing precursors as the sources of elements for the synthesis of g-CNs. Reproduced with permission.[9,10] Copyright 2013 and 2014, Royal Society of Chemistry.

2.2 Synthesis methods of g-CNs

The most common method of synthesizing nano-shaped g-CNs is thermal etching split. This method can create bulk g-CNs that can be broken down into small molecule g-CNs (Fig. 2b). This method can produce very uniform g-CNs and generate different types of g-CN morphologies (such as bulks, sheets, lines, and dots). The "top-down" synthesis method is performed at high-temperature, 825–950 °C. This temperature range can lead to material corrosion.[9] Moreover, because the force between each g-CN layer is relatively weak, bulk g-CNs gradually transform into sheets of g-CNs.

In addition to the "top-down" approach, the "bottom-up" approach can also be used to synthesize g-CNs.[11] This process allows g-CNs to carry a carboxyl group on their surface for subsequent surface functional modification. In 2013, a novel g-CNs-synthesis method was published by Zhang *et al.* (Fig. 2c). This "bottom-up" method used both small molecule carbon precursors (such as sodium citric acid) and small molecule nitrogen precursors (such as urea) and reacted them under hydrothermal conditions to create g-CNs at a high temperature.[10]

3. Diversified applications of graphitic carbon nitride quantum dots

As a new carbon nanomaterial, g-CNs emit a persistent fluorescent signal without a flash. The excitation and emission wavelengths of g-CNs can be adjusted; in addition, the composition of g-CNs leads to their high biocompatibility. This section discusses the reaction mechanism of g-CN fluorescence and focuses on the applications of g-CNs in various fields.

3.1 g-CN QD *in vitro* and *in vivo* bioimaging applications

Due to their limited internal electron motion, g-CNs have significant quantum confinement and edge effects.[13,14] These two size-dependent effects provide g-CNs with new physical and chemical properties when their particle size is less than 10 nm (Fig. 3a). Compared with traditional graphene quantum dots (GQDs), g-CNs have the advantages of low synthesis cost, adjustable energy band gap, and stable photoluminescence quality (Fig. 3b). In addition, their optical tunability allows g-CNs to produce different wavelengths of fluorescence: they emit different wavelengths of blue and green light (Fig. 3c).[15] Therefore, g-CN compounds have huge potential in terms of optoelectronic devices, photocatalysis, and biomedical and other applications (Fig. 3d and e).[12] In terms of their fluorescence performance characteristics, the fluorescence quantum efficiency of g-CNs reaches up to 34.5%. This efficiency is substantially higher than that of traditional GQDs. Clearly, the quantum efficiency (QY%) of g-CNs is sufficient for cell imaging and provides a contrasting image.[16]

3.2 g-CN QD applications in multifunctional biosensing

g-CNs can be used to detect and report on biological molecules due to their unique optical properties.[17] There have been many papers published on this application of g-CNs.[18,19] As biosensors, g-CNs can serve as a nanoplatform to combine biological, physical and chemical factors to detect analytes

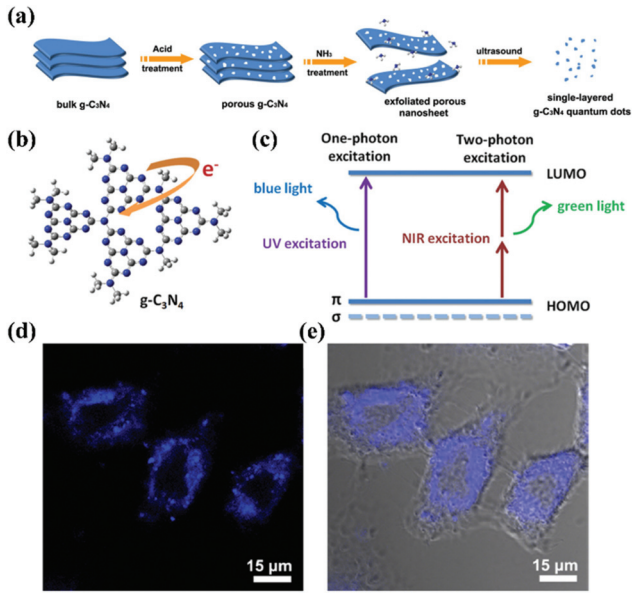

Fig. 3 Biological imaging based on g-CNs luminescence. (a) g-CNs are formed into QDs that have three-dimensional nanostructures using physical and chemical methods, such as acid–base treatment and ultrasound. (b) In g-CNs in the graphitic phase, the tri-triazine structure produces free electrons on their surface. (c) Fluorescence can be achieved using different excitation frequencies that excite blue and green light with single photons and multiple photons, respectively. (d) g-CNs under a conjugated focus microscope emit blue light. Reproduced with permission.[12] Copyright 2014, Wiley Online Library.

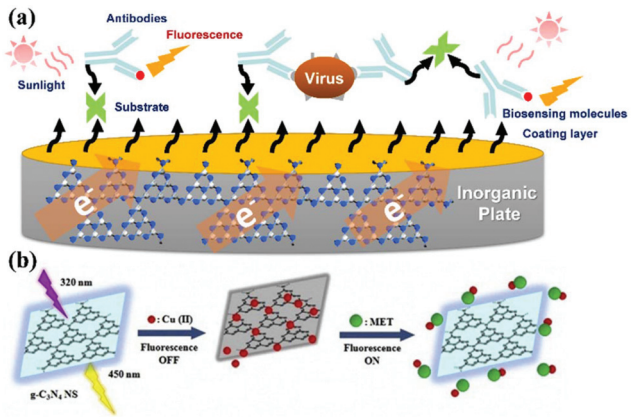

Fig. 4 g-CNs can be used in biological sensing devices for inorganic material substrates. (a) g-CNs are a new type of recently discovered fluorescent material. g-CNs do not contain any toxic metal elements and have potential applications in bioimaging, biosensing, among other applications. Detection of heavy metals using g-CN fluorescent probes is desirable in several applications, such as ions, explosives, biomolecules, and bioimaging. (b) Copper ions are bound to the inorganic plane of g-CNs. Fluorescence imaging can be used to detect different biomolecules. In addition, quantification of the fluorescence intensity can be used to effectively monitor the concentration of biomolecules. Reproduced with permission.[21] Copyright 2018, Elsevier.

(Fig. 4a).[20] Among these factors, biosensors must include the following three features: 1. the ability to carry sensitive biological elements (a biological material, such as tissue, or biological small molecules, such as cell receptors, enzymes, antibodies, and nucleic acids); 2. the ability to connect multiple types of detection methods (*via* optical, electrochemical, temperature and other physical and chemical means or magnetic processes); and 3. the ability to assemble with other platforms (a good platform can combine biological-, physical- and chemical-based factors, such as our topic: g-CNs). g-CNs not only have a sufficiently sensitive fluorescent signal but also have an easily modifiable surface that can be used as a potential biosensor in the future (Fig. 4b).

3.3 g-CN QD applications for cancer therapy

In physiological metabolism, an oxygen-consuming metabolism is likely to produce by-products, and the oxygen-containing substance with excess electrons are called reactive oxygen species (ROS). ROS include oxygen ions, peroxide and oxygen free radicals.[22] These particles are quite small, and due to the presence of unpaired free electrons, ROS are also very active. High levels of ROS will cause cell and gene structure damage (Fig. 5a). Active oxygen, which is an oxygen-containing molecule, contains oxygen ions and hydrogen peroxide. In addition to their roles in cell signaling and homeostasis, ROS have significant side effects. ROS can block the electron transport chain in the mitochondria and cause significant cell

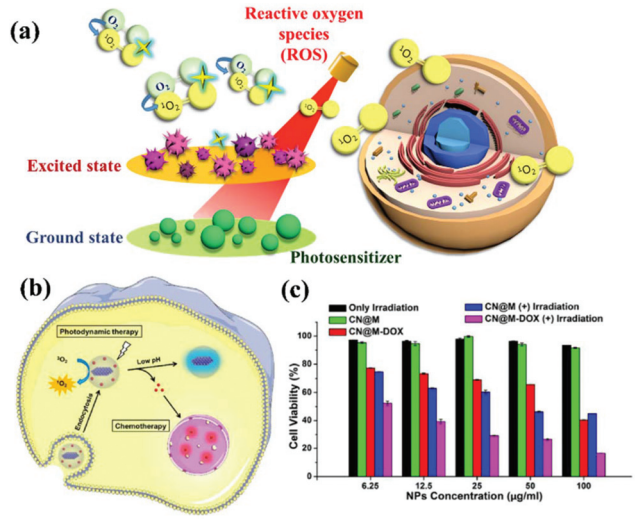

Fig. 5 Process and mechanism of photodynamic therapy. (a) Schematic illustration of g-CN nanosheets as potential photosensitizers for photodynamic therapy (PDT). PDT is a kind of phototherapy. (b) PDT requires three elements: sensitizers, light sources, and oxygen molecules in cells. g-CN nanosheets can include small drug molecules to achieve combined PDT and chemotherapy. (c) g-CNs are a nontoxic photosensitive material that can be made toxic to specific cancer cells or diseased cells *via* exposure to light of a specific wavelength to achieve therapeutic effects. Reproduced with permission.[25] Copyright 2015, Royal Society of Chemistry.

damage.[23] This phenomenon is also known as oxidative stress. Due to these characteristics, some scientists have used oxidative stress damage to treat diseases. This method of using

ROS to inhibit the growth of cancer cells is called photodynamic therapy (PDT).[24] According to the literature, carbon-based materials, such as graphene and its derivatives (for example, graphene oxide), have shown significant potential for biomedical applications, especially DNA detection, bioimaging, drug delivery, and PDT.

Similar to other carbon nanomaterials, g-CNs also exhibit significant photodynamic activity, absorbing the energy of ultraviolet light and producing oxygen free radicals in the environment. Therefore, Li and Yang *et al.* reported that g-CN nanosheets are potential photosensitizers and can be used as pH-responsive drug nanocarriers for cancer treatment (Fig. 5b). In PDT, g-CNs function as a PS to produce ROS under irradiation at the appropriate wavelength.[26] In PDT, the environment is under greater oxidative stress, which affects the cell's electron transport chain and kills cancer cells. Most PSs have some application limitations compared to g-CNs, such as poor water solubility, photobleaching and high toxicity (Fig. 5c). Therefore, g-CNs can be effectively used as novel drug nanocarriers. However, the absorption spectrum of g-CNs is in the UV region and biological tissue has a high absorption capacity for UV light. In addition, high-energy ultraviolet light causes damage to human tissue. These factors suggest that g-CNs are not suitable for use in biological treatment alone. Therefore, although g-CNs have great potential, their application in biomedicine is still limited.

3.4 g-CN QDs for other biological applications

As described above, reactive oxygen species can be used in photodynamic therapy. g-CNs can act as antibacterial materials and convert humic acid into CO_2 and H_2O.[27] This feature allows the application of g-CNs to be extended to infectious diseases and inflammatory diseases.

Zhang *et al.* used g-CNs as an antiviral photocatalyst with a response surface methodology to avoid the serious risk of waterborne viruses. After visible light illumination, the viruses could be completely inactivated by g-CNs without regrowth.[29] The ability of g-CNs to sense oxidative stress is also applied to inflammatory reactions. Liu *et al.* developed based on polydopamine-quenched fluorescent g-CNs for assessing the antioxidant capacity of biological fluids, using the fluorescence "on–off" state of g-CNs to track the presence of antioxidants.[30] In addition to creating oxidative stress to promote cancer cell or bacterial death, g-CNs can also act as a catalyst in the photosynthetic process of plants.[31] g-CNs can catalyze pyruvate conversion into L-lactate in the chloroplast. The authors suggest that g-CNs can be applied to photocatalytic NADH regeneration for internal enzymatic synthesis. When the substrate is present in the environment, g-CNs can absorb light energy to convert NADH into NAD^+.[32–34] L-Lactate dehydrogenase can use this energy to convert pyruvate into L-lactate. As a biological source of hydrogen, NADH is a critical cofactor that participates in many enzymatic hydrogenations with resultant oxidation to NAD^+. g-CNs showed remarkably improved capability in visible light harvesting and exhibited high performance in photocatalytic regeneration with an NADH regeneration yield of up to 40%.[35] Based on the previous statement, an increasing amount of research has been carried out to investigate different biological applications of g-CNs.[36] In the following sections, we will carefully explore how nanocomposites based on g-CNs can achieve better biological applications.[37,38]

4. Applications of graphitic carbon nitride nanocomposites

4.1 g-CN-based biosensors with inorganic materials

g-CN nanosheets are a versatile material platform that can carry a variety of cationic metals, such as Pt, Ag, and Cu, and can use the different properties of these cations to detect specific molecules in the environment. Table 1 lists various biosensors combined with g-CN nanosheets, which are organized according to year and function. g-CNs as biosensors are divided into electrochemical biosensors (ECL)[39–49] and persistent luminescence (PL)[17,21,50–53] biosensors and electrochemical biosensors can be used for biological or chemical sensing. An electrochemical signal can be converted into an electronic signal, and the intensity of this signal is proportional to the concentration of the analyte. Optical sensors use light-sensitive elements to convert optical signals into sensors for use in telecommunications. The most common currently used photosensitive elements sense wavelengths near the wavelength of visible light, such as infrared wavelengths and ultraviolet wavelengths. Sensors are used not only to measure light but also to sense the light signal. Often, a detector is used as a type of sensor to detect nonelectricity (such as temperature) and convert nonelectricity into optical signal changes. Currently, a combination of two detection mechanisms, photoelectrochemical (PEC) biosensing, is used, which can verify the concentration of the analyte using both electrical and optical methods simultaneously.[54–60]

4.1.1 g-CN-based biosensors with electrochemiluminescence (ECL) properties. Electrochemiluminescence (ECL) or electrochemical chemiluminescence is the luminescence that occurs during an electrochemical reaction in solution. In electroluminescent chemiluminescence, electrochemically produced intermediates undergo a highly exergonic reaction to produce an electronically excited state that illuminates when relaxed to a lower level. This wavelength of the emitted photons corresponds to the energy gap between the two states. ECL excitation can be caused by high energy electron transfer (redox) reactions of electroformed materials. A luminescent excitation is a form of chemiluminescence in which one/all of the reactants are electrochemically produced on the electrode. Moreover, g-CNs have a large specific surface area, so they can provide more sites to separate charge carriers, reduce the recombination rate of the charge carriers and further increase the activity of the reduction reaction. Second, g-CNs have high electron conductivity, which means that they can effectively separate and transfer charge carriers when exposed to ultraviolet and visible light, thereby improving the electronic properties of the entire system. Thus, highly conductive nano-

Table 1 Summary of g-CN-based biosensors. Biosensors combining various inorganic nanomaterials with g-CNs are listed in the table. According to the literature, various detection molecules and detection limits are compiled

Metal ions	Biological targets	Detection methods	Limit of detection	Ref.
Silver nanomaterials (Ag)	Glutathione (GSH)	Persistent luminescence	9.6 nM	2013, Tang *et al.*[17]
	$S_2O_8^{2-}$	Electrochemiluminescence	0.0003 ng mL^{-1}	2016, Fan *et al.*[39]
	DNA	Persistent luminescence	1.0 nM	2017, Xiao *et al.*[50]
AgI/ITO	Cancer cell	Photoelectrochemical	5 cells per mL	2018, Mazhabi *et al.*[54]
Gold nanomaterials (Au)	Lactate	Electrochemiluminescence	5.5 nM	2014, Chen *et al.*[48]
	DNA	Electrochemiluminescence	50 attomolar	2017, Rasheed *et al.*[42]
Au/Gox	Glucose	Electrochemiluminescence	0.05 μM	2017, Jiang *et al.*[43]
Au/Cu	Sudan I	Electrochemiluminescence	0.17 pg mL^{-1}	2018, Chen *et al.*[40]
Iron nanomaterials (Fe)	Organophosphate pesticide (OP)	Electrochemiluminescence	0.3 pM	2016, Wang *et al.*[49]
CdS-quantum dots				
CdS/Ppy	Adenosine	Photoelectrochemical	0.1 nmol L^{-1}	2016, Liu *et al.*[55]
CuxS-doped CdS	RNA	Photoelectrochemical	3.53 pM	2017, Wang *et al.*[57]
CdS and Ag	u-Plasminogen activator	Photoelectrochemical	33 fg mL^{-1}	2018, Liu *et al.*[56]
Copper nanomaterials (Cu)	Alkaline phosphatase (ALP)	Persistent luminescence	0.08 U L^{-1}	2016, Xiang *et al.*[51]
	DNA	Electrochemiluminescent	3.6×10^{-14} M	2017, Ji *et al.*[44]
	Metformin	Persistent luminescence	0.003 μM	2018, Rahbar *et al.*[21]
CuO	Dopamine	Electrochemiluminescent	10^{-10} mol L^{-1}	2018, Zou *et al.*[45]
Palladium (Pd)	OPs and HupA	Electrochemiluminescence	0.67 nM	2016, Wang *et al.*[46]
Platinum (Pt)	Hg^{2+}	Persistent luminescence	1.23 nM	2017, Wang *et al.*[53]
TiO_2	Thrombin	Photoelectrochemical	1.2×10^{-13} mol L^{-1}	2016, Fan *et al.*[60]
	Protein kinase	Photoelectrochemical	0.048 U mL^{-1}	2017, Li *et al.*[59]
TiO_2 and N-GQD	pcDNA3-HBV	Persistent luminescence	0.005 fmol L^{-1}	2017, Pang *et al.*[58]
ZnO	Sulfamethoxazole (SMZ)	Electrochemiluminescence	5.78 nM	2018, Balasubramanian *et al.*[47]

particles (silver, Ag nanoparticles) supported on g-CNs are under development for use as ECL biosensors. For instance, Fan *et al.* designed a novel "on–off" ECL biosensor by conjugating g-CNs with Ag-doped g-CN nanosheets.[39]

Thus, ECL emissions can be generated as described in eqn (1)–(9). The possible ECL mechanism of Ag–g-CN with $S_2O_8^{2-}$ as the co-reactant is shown. As a result, strong ECL signals can be produced and achieve "on–off" biosensors.

$$\text{Ag–g-CN} + e^- \rightarrow \text{Ag–g-CN}^{\bullet -} \quad (1)$$

$$O_2 + 2H_2O + 2e^- \rightarrow 2H^2O^2 \quad (2)$$

$$H_2O_2 + e^- \rightarrow OH^- + OH^- \quad (3)$$

$$OH^- + \text{Ag–g-CN}^{\bullet -} \rightarrow \text{Ag–g-CN}^* + OH^- \quad (4)$$

$$S_2O_8^{2-} + e^- \rightarrow SO_4^{2-} + SO_4^- \quad (5)$$

$$\text{Ag–g-CN}^{\bullet -} + SO_4^- \rightarrow \text{Ag–g-CN}^* + SO_4^{2-} \quad (6)$$

and/or

$$\text{Ag–g-CN}^{\bullet -} + SO_4^- \rightarrow \text{Ag–g-CN}^+ + SO_4^{2-} \quad (7)$$

$$\text{Ag–g-CN}^+ + \text{Ag–g-CN}^{\bullet -} \rightarrow \text{Ag–g-CN}^* + \text{Ag–g-CN} \quad (8)$$

Finally,

$$\text{Ag–g-CN}^* \rightarrow \text{Ag–g-CN} + h\nu. \quad (9)$$

4.1.2 g-CN-based biosensors with persistent luminescence (PL) properties. Persistent luminescence (PL), often referred to as phosphorescence and/or fluorescence, is a long-lasting luminescence phenomenon encountered in materials that causes them to illuminate in the dark after excitation with UV or visible light. The reason for PL is that de-excitation between the two electronic states has different spin multiplicities. For continuous illumination, this phenomenon has long been known to involve energy traps (*e.g.*, electron or hole traps) in the material that are filled during excitation. After the excitation, the stored energy is gradually released to the center of the emitter, which typically illuminates through a fluorescence-like mechanism. Since two-dimensional (2D) carbon-based nanomaterials have received a large amount of attention in recent years because they exhibit unusual physical properties due to the quantum size effects associated with their ultrathin nature, several g-CN-based fluorescence sensing strategies have been developed for the detection of biomolecules with various inorganic nanoparticles, such as Cu^{2+}, Ag^+, Fe^{3+}, and Cr^{3+}. Moreover, the use of g-CNs as biological nanoprobes has already been extended to bioimaging and immunoassays. Additionally, Cu^{2+}-mediated g-CN fluorescent nanocomposites have been developed by Liu *et al.*[52] In the presence of Cu^{2+}, the fluorescence of g-CNs is quenched by Cu^{2+}. When adding adenosine 5′-diphosphatesodium salt (ADP) to the solution, ADP interacts with Cu^{2+}, which weakens the interaction between Cu^{2+} and g-CNs, leading to a slight recovery of the quenched fluorescence of g-CNs. There is also a photoinduced electron transfer (PET) biological detection method.

4.1.3 g-CN-based biosensors with photoelectrochemical (PEC) properties. Photoelectrochemical (PEC) processes are promising, low-cost methods for converting chemical energy into electrical energy under illumination at applied potentials. PEC biosensing has attracted a large amount of attention due to its ability to detect biomolecules by the photocurrents gen-

erated by biomolecular oxidation. In a PEC sensor, a series of charge transfer processes must occur between the analyte and photocatalytic material. Thus, g-CNs can be combined with inorganic materials to effectively utilize the output photocurrent. Therefore, the design of the photoelectronic biosensor and manipulation of electron capture and transmission are important features that define the overall efficiency of the PEC sensor. For example, a novel photoelectrochemical (PEC) assay has been developed for the sensitive detection of protein kinase A (PKA). The g-CNs and titanium dioxide (TiO_2) nanocomposite have been synthesized and characterized, and it provides a PEC signal due to the ability of TiO_2 to conjugate phosphate groups and g-CNs. The properties of this g-CNs photoactive material allow the detection of PKA activity. Li *et al.* developed a simple and sensitive PEC strategy for detecting PKA activity based on combining the PKA-catalyzed phosphorylation reaction in solution with signal amplification *via* poly(amidoamine) dendrimer (PAMAM) and ALP.[59] TiO_2 can specifically bind to substrate peptides. Thus, peptides can be captured on the surface of TiO_2/g-CN/ITO. Because a specific peptide can be immobilized on TiO_2/g-CN nanoparticles, the quantity of the immobilized peptide will increase with PKA activity.

4.2 g-CN-based biotherapy with inorganic nanomaterials

Photodynamic therapy (PDT) is based on the production of reactive oxygen species (ROS) to damage organelles, tissues or organs.[24,25] Briefly, PDT is an emerging therapeutic modality that uses photosensitizers (PSs) and light irradiation to eradicate cancer tissues.[61] Under appropriate light excitation, PSs can interact with molecular oxygen and generate cytotoxic singlet oxygen ($^1O_2$), which kills cancer cells. Traditionally, most PSs can be excited by only UV or visible light. Although g-CNs have several advantages, such as a mild band gap (2.7 eV), the ability to absorb visible light and flexibility, they still have limitations for practical applications due to their low efficiency of visible light utilization and low UV light penetration depth. To modify these limitations, one of the most attractive approaches is combining g-CNs with other high-performance nanomaterials, such as lanthanide-doped upconversion nanoparticles (UCNPs).[62] The author proposes to enhance the PDT effect by providing more electron transfer *via* Cu, which greatly improved the original PDT capability (Fig. 6a). When Cu and g-CNs are simultaneously irradiated with a UV light source, the combination with Cu is obviously better than pure g-CNs (Fig. 6b).[28] However, the author also mentions that UV and visible light are not suitable excitation wavelengths for biotherapeutics. Thus, g-CNs could be tuned to emit in other spectral regions if suitably coupled with lanthanide ions.[63,64] Recently, lanthanide-doped UCNPs have received increasing attention for use in a variety of biological applications due to their ability to convert NIR light to visible light.[65,66] Along with their remarkable light penetration depth and the absence of autofluorescence in biological specimens under NIR excitation, these UCNPs have shown great promise as photosensitizing nanoplatforms in NIR-triggered PDT to overcome the

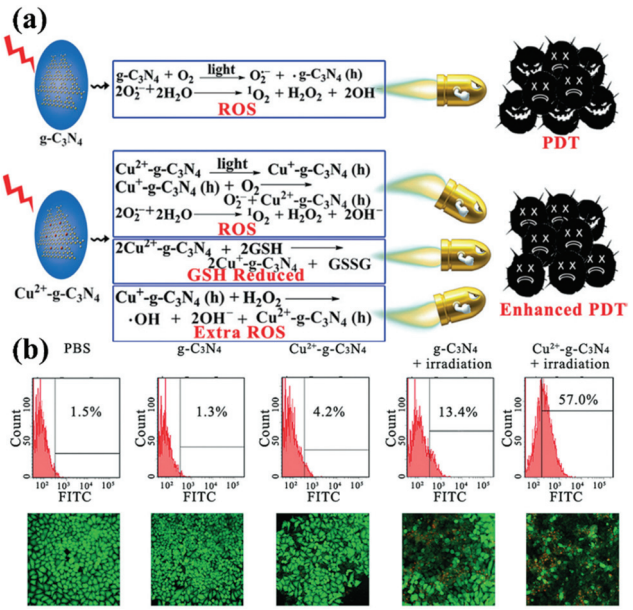

Fig. 6 g-CNs combine with copper ions to form a highly efficient photodynamic sensitizer. (a) Copper ions can interact with GSH and reduce the activity of GSH, which makes it difficult for cells to restore ROS. Excess ROS can increase oxidative stress in cells and enhance the effects of PDT. (b) As seen from the flow cytometry results, pure PBS, g-CNs and copper ions do not cause damage to cells. When illuminated, g-CNs produce ROS that attack cells. When combined with copper ions, the effect of PDT can be significantly improved. Reproduced with permission.[28] Copyright 2016, Wiley Online Library.

drawbacks of g-CNs under UV/visible light.[68] The authors used iron nanoparticles and UCNPs and coated g-CNs to give the material both fluorescence, magnetic and therapeutic functions.[69] In addition to the change in the excitation wavelength, the authors used gold nanoclusters (Au_{25}) to improve the PDT effect (Fig. 7a).[67] Due to the excellent valence band of the gold nanoclusters, the absorption spectrum of g-CNs is consistent with the emission spectrum of gold nanoclusters (Fig. 7b). The therapeutic effect of g-CNs is enhanced by the surface plasma resonance (SPR) effect (Fig. 7c).[67]

In addition, current research on g-CNs has led to advanced diagnoses and treatments. Chan *et al.* proposed the incorporation of rare earth, neodymium ions (Nd^{3+}) in UCNPs. Nd^{3+} has cross-strong absorption at 808 nm, so the excitation source of UCNPs could shift to 808 nm and solve the problem of heat.[70] This 808 nm NIR biological window not only avoids the absorption of water but also enhances the penetration depth up to 30 mm. Since 808 nm-excited UCNPs can generate more photons, the power of the NIR laser for both groups is the same, 1 W cm^{-2}, except that the two groups use lasers at different wavelengths 980 nm and 808 nm. By detecting the blue fluorescence of UCNP at 474 nm, it was found that the 808 nm group generated 6.23×10^9 photons, and the 980 nm group generated only 5.1×10^9 photons (Fig. 8b).

Based on this result, 808 nm-excited UCNPs can transfer a large amount of energy to g-CNs and induce green fluo-

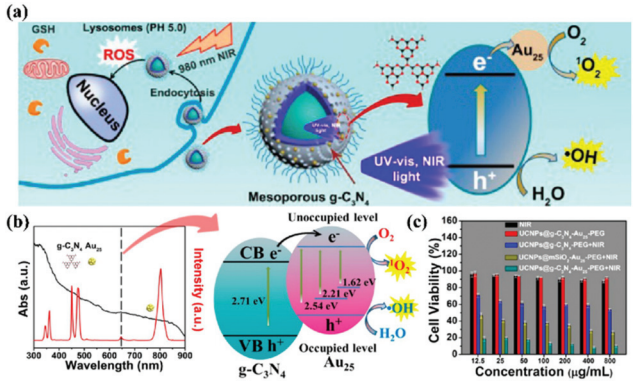

Fig. 7 Improving the excitation light conditions of g-CNs optimizes PDT. (a) g-CNs combined with UCNPs changes the excitation source to near-infrared light and can be combined with the Jinnai cluster to improve the effect of PDT. (b) g-CNs and Au_{25} have overlapped absorption and luminescence, both of which effectively absorb the light emitted by UCNPs. The difference in the energy levels between g-CNs and Au_{25} can expand the transition of electrons, convert O_2 to O_2^- and convert H_2O to OH^-. (c) When g-CNs are combined with Au_{25}, the photodynamic effect is significantly improved. Significant differences can be obtained through biotoxicity testing. Reproduced with permission.[67] Copyright 2017, American Chemical Society.

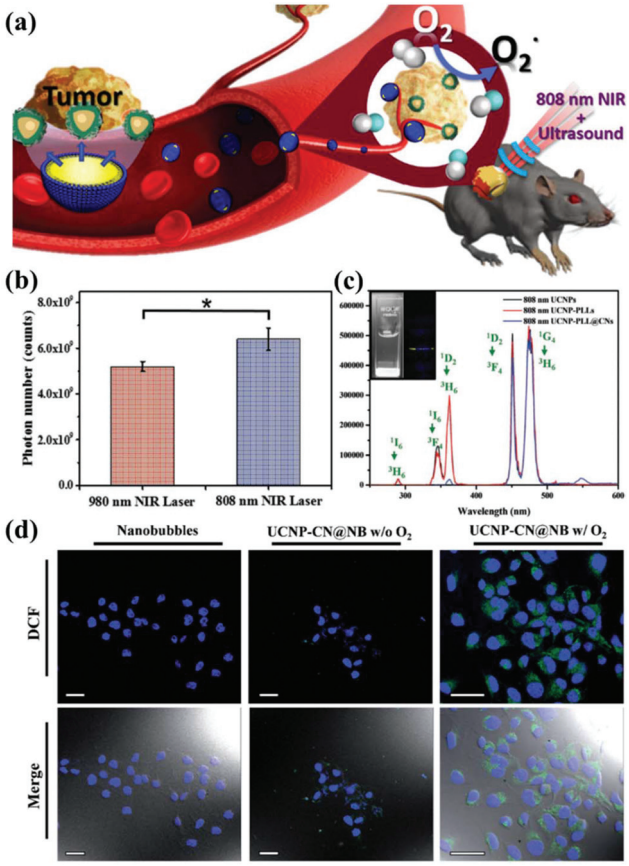

Fig. 8 g-CN-based biotherapy with UCNPs. (a) g-CNs combined with 808 nm-excited UCNPs and nanobubbles to form advanced theranostic nanoplatforms. (b) Photon quantification of UCNP@CN bioluminescence images with 980 nm and 808 nm NIR irradiation. (c) Photoluminescence spectra of 808 nm-excited UCNP-PLL@CNs (inset: the digital fluorescence photographs of nanocomposites have both blue and green fluorescence). Reproduced with permission.[70] Copyright 2017, Wiley Online Library. (d) Tumor cells treated with UCNP-CN@NBs (500 μg mL^{-1}) are exposed to an 808 nm laser. The cells were stained with DCF detection dye. An increase in green fluorescence in irradiated cells indicates ROS production. Reproduced with permission.[71] Copyright 2018, Royal Society of Chemistry.

rescence (emitted from g-CNs), which is detected in the photoluminescence spectrum (Fig. 8c). Except for adjusting the choice of the excitation source, Chan *et al.* also focused on the PDT effect caused by g-CNs.[71] Although PDT shows some outstanding therapeutic advantages, it still has some problems that need to be solved. First, the light penetration depth is still not deep enough to penetrate organs in the human body.[73] Second, commonly used organic materials have poor stability.[74] Third, the hypoxic environment that commonly surrounds cancer cells still needs to be discussed in future research because hypoxic environments may strongly affect the PDT effect generated by g-CNs (Fig. 8a).[75] Therefore, mixing oxygen in an organic nanoscale carrier, such as a lipid nanobubble, to increase ROS production can relieve the hypoxic state surrounding cancer cells. In this study, the 2′,7′-dichlorofluorescein diacetate (H2-DCFDA) reagent was used to detect ROS production in cells. The H2-DCFDA reagent is not a fluorescent dye and is free to pass through the cell membrane. When the H2-DCFDA reagent enters the cytosol, it can encounter a lipolytic enzyme called intracellular esterase and be hydrolyzed to 2′,7′-dichlorofluorescein (DCFH). DCFH cannot penetrate the cell membrane. Therefore, DCFH remains in the cytosol.

When ROS are present in the cellular environment, DCFH will be oxidized to the fluorescent dye DCF. The detection principle is based on DCF detection, which emits green fluorescence, allowing the amount of ROS in the cells to be determined. After 10 minutes of laser irradiation, UCNP-CN@NBs with O_2 and no O_2 produced green fluorescence. In addition, UCNP-CN@NBs with O_2 produce more ROS than UCNP-CN@NBs without O_2, which can be distinguished by the combined result in the bright field. These results indicate that the use of g-CNs loaded in nanobubbles is a successful and intelligent design for producing better PDT results through oxygen loading (Fig. 8d).

4.3 g-CN-based wound healing

Nanocomposite technology continues to advance. In addition to being a biosensor and photosensitizer, g-CNs can be combined with Zn^{2+} and graphite oxide (GO) to form a composite (Fig. 9a). The antibacterial effect of this composite is also achieved in the form of ROS, which makes wounds easier to heal. The authors propose to reduce bacterial growth on the wound surface by irradiating the wound with light at two wavelengths. Combining the PDT effect provided by g-CNs with the photothermal treatment of GO causes bacteria to die faster and accelerates wound healing (Fig. 9b).[72]

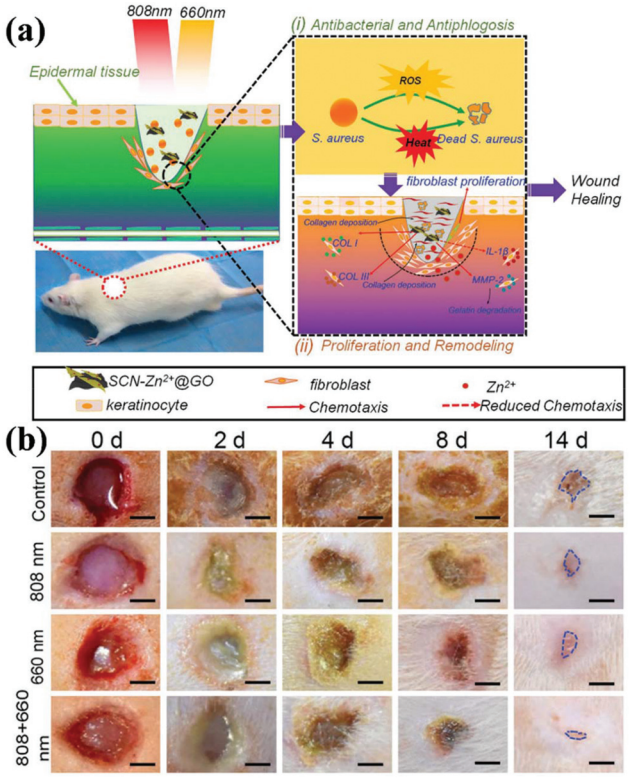

Fig. 9 Wound healing g-CNs combine with Zn^{2+} and graphene oxide to form a highly effective antibacterial agent. (a) Wound healing is affected by a bacterial infection, associated inflammation, cell proliferation and differentiation, and tissue remodeling. Current antibiotic treatments do not simultaneously promote wound healing and kill bacteria. g-CNs are complexed with Zn^{2+} and graphene oxide (GO), and two different excitation, at 660 and 808 nm, can be used for wound disinfection. This strategy allows Zn^{2+} and GO modifications on g-CNs. The antibacterial action of ROS accelerates wound healing at the same time, which makes g-CN-Zn^{2+}@GO very promising for the treatment of bacterial wounds and wound healing. (b) The results are shown at 2, 4, 8 and 14 days (blue lines indicate wound shape at 14 days). Secretion and pus reduction were observed under mixed light illumination compared to the control (dark treatment) and individual light irradiation (660 or 808 nm) groups after 2 days. Reproduced with permission.[72] Copyright 2018, Wiley Online Library.

5. Conclusions and prospects

In the past few years, graphene-like 2D nanomaterials (including our topic, g-CN nanomaterials) have been widely used as electron donors and have extended research in this field to organisms. The broad use of g-CNs can be attributed to their unique 2D structure, large area to volume ratio, tunable band, and good optical properties. In this review, we describe the optical properties of g-CN nanomaterials as well as recent developments in these nanomaterials in combination with other nanoparticles. From imaging, biosensing and PDT effects, g-CNs reveal their advantages for biological applications. We first discuss the development of a luminescence analysis based on g-CN nanomaterials. Further studies are needed to more deeply explore g-CNs, such as determining their optical properties, developing new biofunctional strategies, improving their dispersibility in water, and reducing their toxicity to organisms. In terms of current research, g-CNs are an excellent biosensing platform. g-CNs can measure a wide range of indicator molecules and synergize with other nanomaterials to improve their sensitivity. Moreover, we focus on whether other nanomaterials can transfer their unique characteristics to g-CNs and form multifunctional nanocomposites. However, g-CNs still have many challenges that need to be overcome. The first challenge is the optical issue. Although g-CNs have a suitable energy band (2.7 eV) to provide blue fluorescence emission, the structure of g-CNs is stable and difficult to modify, which means that the energy band of g-CNs is difficult to adjust and that their absorption is located in the ultraviolet region. Their excitation in the ultraviolet region has inspired researchers to find ways to improve this drawback, such as combining g-CNs with UCNPs. This nanocomposite allows g-CNs to achieve perform better as a photodynamic photosensitizer, but some questions have emerged. As a photosensitizer, can a stable nanomaterial such as g-CNs be smoothly excluded from living organisms? In addition, although the composition of g-CNs only contains C and N, the biological toxicity still needs to be evaluated if it accumulates in a large amount. Because the composition of g-CNs is simple, these toxicity-related issues have rarely been studied, but they still require more attention. In our opinion, further work should address the following: (1) although g-CNs have optical tunability, they are still limited to the ultraviolet region; (2) g-CNs have good electronic properties, but it still needs to be determined whether the supply capacity of g-CNs can be developed into an integrated biosensing platform that allows the monitoring of multiple indicators of biomolecules; (3) g-CNs can effectively generate free radicals as photosensitizers of PDT; however, their conversion efficiency still needs to be evaluated; and (4) the accumulation and toxicity of g-CNs may require a comprehensive assessment. In summary, various types of g-CN nanocomposite systems have been designed and configured in many research articles. g-CNs can be used with other nanocomposite systems to provide unique properties in photocatalytic applications and enhance the performance of other nanocomposites. In addition, g-CN nanocomposites can be applied to biological organisms as a component of sensors or as biomedical platforms. It is speculated that research interest in g-CN nanocomposites will increase in the future.

Conflicts of interest

The authors have no existing conflicts to declare.

Acknowledgements

This research was supported by Academia Sinica [AS-SUMMIT-108] to MH and Academia Sinica Joint Program

Office [AS-NTU-108-01 to MH and NTU-AS-108L104301 to RSL]. Moreover, the authors would like to thank the Ministry of Science and Technology financial support [MOST 107-2113-M-002-008-MY3] to RSL.

References

1 F. Tian, J. Lyu, J. Y. Shi and M. Yang, *Biosens. Bioelectron.*, 2017, **89**, 123–135.
2 F. Zhao, Z. Li, L. X. Wang, C. G. Hu, Z. P. Zhang, C. Li and L. T. Qu, *Chem. Commun.*, 2015, **51**, 13201–13204.
3 G. Algara-Siller, N. Severin, S. Y. Chong, T. Bjorkman, R. G. Palgrave, A. Laybourn, M. Antonietti, Y. Z. Khimyak, A. V. Krasheninnikov, J. P. Rabe, U. Kaiser, A. I. Cooper, A. Thomas and M. J. Bojdys, *Angew. Chem., Int. Ed.*, 2014, **53**, 7450–7455.
4 A. Thomas, A. Fischer, F. Goettmann, M. Antonietti, J. O. Muller, R. Schlogl and J. M. Carlsson, *J. Mater. Chem.*, 2008, **18**, 4893–4908.
5 J. Liu, H. Q. Wang and M. Antonietti, *Chem. Soc. Rev.*, 2016, **45**, 2308–2326.
6 Y. Q. Dong, Q. Wang, H. S. Wu, Y. M. Chen, C. H. Lu, Y. W. Chi and H. H. Yang, *Small*, 2016, **12**, 5376–5393.
7 J. Oh, R. J. Yoo, S. Y. Kim, Y. J. Lee, D. W. Kim and S. Park, *Chem. – Eur. J.*, 2015, **21**, 6241–6246.
8 Y. Li, Y. Zhao, H. H. Cheng, Y. Hu, G. Q. Shi, L. M. Dai and L. T. Qu, *J. Am. Chem. Soc.*, 2012, **134**, 15–18.
9 W. J. Wang, J. C. Yu, Z. R. Shen, D. K. L. Chan and T. Gu, *Chem. Commun.*, 2014, **50**, 10148–10150.
10 J. Zhou, Y. Yang and C. Y. Zhang, *Chem. Commun.*, 2013, **49**, 8605–8607.
11 L. B. Tang, R. B. Ji, X. K. Cao, J. Y. Lin, H. X. Jiang, X. M. Li, K. S. Teng, C. M. Luk, S. J. Zeng, J. H. Hao and S. P. Lau, *ACS Nano*, 2012, **6**, 5102–5110.
12 X. D. Zhang, H. X. Wang, H. Wang, Q. Zhang, J. F. Xie, Y. P. Tian, J. Wang and Y. Xie, *Adv. Mater.*, 2014, **26**, 4438–4439.
13 X. D. Zhang, X. Xie, H. Wang, J. J. Zhang, B. C. Pan and Y. Xie, *J. Am. Chem. Soc.*, 2013, **135**, 18–21.
14 H. Ding, P. Zhang, T. Y. Wang, J. L. Kong and H. M. Xiong, *Nanotechnology*, 2014, **25**, 205604.
15 Y. H. Zhang, Q. W. Pan, G. Q. Chai, M. R. Liang, G. P. Dong, Q. Y. Zhang and J. R. Qiu, *Sci. Rep.*, 2013, **3**, 1943.
16 J. W. Liu, Y. M. Wang, C. H. Zhang, L. Y. Duan, Z. Li, R. Q. Yu and J. H. Jiang, *Anal. Chem.*, 2018, **90**, 4649–4656.
17 Y. R. Tang, H. J. Song, Y. Y. Su and Y. Lv, *Anal. Chem.*, 2013, **85**, 11876–11884.
18 S. Barman and M. Sadhukhan, *J. Mater. Chem.*, 2012, **22**, 21832–21837.
19 Y. C. Lu, J. Chen, A. J. Wang, N. Bao, J. J. Feng, W. P. Wang and L. X. Shao, *J. Mater. Chem. C*, 2015, **3**, 73–78.
20 Y. T. Liu, Q. B. Wang, J. P. Lei, Q. Hao, W. Wang and H. X. Ju, *Talanta*, 2014, **122**, 130–134.
21 N. Rahbar, P. Abbaszadegan and A. Savarizadeh, *Anal. Chim. Acta*, 2018, **1026**, 117–124.
22 J. Dong, Y. L. Zhao, H. Y. Chen, L. Liu, W. X. Zhang, B. L. Sun, M. F. Yang, Y. Wang and L. F. Dong, *New J. Chem.*, 2018, **42**, 14263–14270.
23 D. Yang, G. X. Yang, S. L. Gai, F. He, C. X. Li and P. P. Yang, *ACS Appl. Mater. Interfaces*, 2017, **9**, 6829–6838.
24 L. S. Lin, Z. X. Cong, J. Li, K. M. Ke, S. S. Guo, H. H. Yang and G. N. Chen, *J. Mater. Chem. B*, 2014, **2**, 1031–1037.
25 R. Chen, J. F. Zhang, Y. Wang, X. F. Chen, J. A. Zapien and C. S. Lee, *Nanoscale*, 2015, **7**, 17299–17305.
26 Z.-X. C. Li-Sen Lin, J. Li, K.-M. Ke, S.-S. Guo, H.-H. Yang and G.-N. Chen, *J. Mater. Chem. B*, 2014, **2**, 1031–1037.
27 S. F. Kang, L. Zhang, M. F. He, Y. Y. Zheng, L. F. Cui, D. Sun and B. Hu, *Carbon*, 2018, **137**, 19–30.
28 E. G. Ju, K. Dong, Z. W. Chen, Z. Liu, C. Q. Liu, Y. Y. Huang, Z. Z. Wang, F. Pu, J. S. Ren and X. G. Qu, *Angew. Chem., Int. Ed.*, 2016, **55**, 11467–11471.
29 C. Zhang, Y. Li, W. L. Zhang, P. F. Wang and C. Wang, *Chemosphere*, 2018, **195**, 551–558.
30 J. J. Liu, Z. T. Chen, Z. Zhong, X. M. Yan, L. T. Kang and J. N. Yao, *Sens. Actuators, B*, 2018, **262**, 570–576.
31 J. H. Huang, M. Antonietti and J. Liu, *J. Mater. Chem. A*, 2014, **2**, 7686–7693.
32 J. Liu and M. Antonietti, *Energy Environ. Sci.*, 2013, **6**, 1486–1493.
33 J. Liu, R. Cazelles, Z. P. Chen, H. Zhou, A. Galarneau and M. Antonietti, *Phys. Chem. Chem. Phys.*, 2014, **16**, 14699–14705.
34 J. Liu, J. H. Huang, H. Zhou and M. Antonietti, *ACS Appl. Mater. Interfaces*, 2014, **6**, 8434–8440.
35 D. Yang, H. J. Zou, Y. Z. Wu, J. F. Shi, S. H. Zhang, X. D. Wang, P. P. Han, Z. W. Tong and Z. Y. Jiang, *Ind. Eng. Chem. Res.*, 2017, **56**, 6247–6255.
36 A. Hayat, J. Khan, M. U. Rahman, S. B. Mane, W. U. Khan, M. Sohai, N. U. Rahman, N. Shaishta, Z. G. Chi and M. M. Wu, *J. Colloid Interface Sci.*, 2019, **548**, 197–205.
37 Y. J. Chung, B. I. Lee, J. W. Ko and C. B. Park, *Adv. Healthcare Mater.*, 2016, **5**, 1560–1565.
38 Z. W. Zhao, Y. J. Sun and F. Dong, *Nanoscale*, 2015, **7**, 15–37.
39 Y. Fan, X. R. Tan, X. Ou, Q. Y. Lu, S. H. Chen and S. P. Wei, *Electrochim. Acta*, 2016, **202**, 90–99.
40 W. L. Chen, X. Yao, X. C. Zhou, K. Zhao, A. P. Deng and J. G. Li, *Microchim. Acta*, 2018, **185**, 275.
41 G. X. Li, X. X. Yu, D. Q. Liu, X. Y. Liu, F. Li and H. Cui, *Anal. Chem.*, 2015, **87**, 10976–10981.
42 P. A. Rasheed, T. Radhakrishnan, S. R. Nambiar, R. T. Thomas and N. Sandhyarani, *Sens. Actuators, B*, 2017, **250**, 162–168.
43 J. J. Jiang, D. Chen and X. Z. Du, *Sens. Actuators, B*, 2017, **251**, 256–263.
44 J. J. Ji, J. Wen, Y. F. Shen, Y. Q. Lv, Y. L. Chen, S. Q. Liu, H. B. Ma and Y. J. Zhang, *J. Am. Chem. Soc.*, 2017, **139**, 11698–11701.
45 J. Zou, S. L. Wu, Y. Liu, Y. J. Sun, Y. Cao, J. P. Hsu, A. T. S. Wee and J. Z. Jiang, *Carbon*, 2018, **130**, 652–663.

46 B. X. Wang, C. Ye, X. Zhong, Y. Q. Chai, S. H. Chen and R. Yuan, *Electroanalysis*, 2016, **28**, 304–311.
47 P. Balasubramanian, R. Settu, S. M. Chen and T. W. Chen, *Microchim. Acta*, 2018, **185**, 396.
48 H. M. Chen, X. R. Tan, J. J. Zhang, Q. Y. Lu, X. Ou, Y. Ruo and S. H. Chen, *RSC Adv.*, 2014, **4**, 61759–61766.
49 B. X. Wang, H. J. Wang, X. Zhong, Y. Q. Chai, S. H. Chen and R. Yuan, *Chem. Commun.*, 2016, **52**, 5049–5052.
50 Y. Xiao, Y. H. Sheng, J. Zhou, M. M. Chen, W. Wen, X. H. Zhang and S. F. Wang, *Analyst*, 2017, **142**, 2617–2623.
51 M. H. Xiang, J. W. Liu, N. Li, H. Tang, R. Q. Yu and J. H. Jiang, *Nanoscale*, 2016, **8**, 4727–4732.
52 L. Liu, J. W. Liu, L. Y. Duan, F. Y. Luo, Y. M. Wang, R. Q. Yu and J. H. Jiang, *Sens. Actuators, B*, 2018, **267**, 231–236.
53 Y. W. Wang, L. X. Wang, F. P. An, H. Xu, Z. J. Yin, S. R. Tang, H. H. Yang and H. B. Song, *Anal. Chim. Acta*, 2017, **980**, 72–78.
54 R. M. Mazhabi, L. Q. Ge, H. Jiang and X. M. Wang, *J. Mater. Chem. B*, 2018, **6**, 5039–5049.
55 Y. X. Liu, H. M. Ma, Y. Zhang, X. H. Pang, D. W. Fan, D. Wu and Q. Wei, *Biosens. Bioelectron.*, 2016, **86**, 439–445.
56 X. P. Liu, J. S. Chen, C. J. Mao, H. L. Niu, J. M. Song and B. K. Jin, *Anal. Chim. Acta*, 2018, **1025**, 99–107.
57 H. Y. Wang, Q. H. Zhang, H. S. Yin, M. H. Wang, W. J. Jiang and S. Y. Ai, *Biosens. Bioelectron.*, 2017, **95**, 124–130.
58 X. H. Pang, H. J. Bian, W. J. Wang, C. Liu, M. S. Khan, Q. Wang, J. N. Qi, Q. Wei and B. Du, *Biosens. Bioelectron.*, 2017, **91**, 456–464.
59 X. Li, L. S. Zhu, Y. L. Zhou, H. Yin and S. Y. Ai, *Anal. Chem.*, 2017, **89**, 2369–2376.
60 D. W. Fan, C. J. Guo, H. M. Ma, D. Zhao, Y. N. Li, D. Wu and Q. Wei, *Biosens. Bioelectron.*, 2016, **75**, 116–122.
61 C. F. Chan, Y. Zhou, H. Y. Guo, J. Y. Zhang, L. J. Jiang, W. Chen, K. K. Shiu, W. K. Wong and K. L. Wong, *ChemPlusChem*, 2016, **81**, 535–540.
62 W. Wang, M. M. Wu and G. K. Liu, *Spectrosc. Lett.*, 2007, **40**, 259–269.
63 P. A. Tanner, L. Zhou, C. K. Duan and K. L. Wong, *Chem. Soc. Rev.*, 2018, **47**, 5234–5265.
64 J. X. Zhang, W. L. Chan, C. Xie, Y. Zhou, H. F. Chau, P. Maity, G. T. Harrison, A. Amassian, O. F. Mohammed, P. A. Tanner, W. K. Wong and K. L. Wong, *Light: Sci. Appl.*, 2019, **8**, 259–269.
65 L. L. Feng, F. He, B. Liu, G. X. Yang, S. L. Gai, P. P. Yang, C. X. Li, Y. L. Dai, R. C. Lv and J. Lin, *Chem. Mater.*, 2016, **28**, 7935–7946.
66 Z. Y. Hou, Y. X. Zhang, K. R. Deng, Y. Y. Chen, X. J. Li, X. R. Deng, Z. Y. Cheng, H. Z. Lian, C. X. Li and J. Lin, *ACS Nano*, 2015, **9**, 2584–2599.
67 L. L. Feng, F. He, Y. L. Dai, B. Liu, G. X. Yang, S. L. Gai, N. Niu, R. C. Lv, C. X. Li and P. P. Yang, *ACS Appl. Mater. Interfaces*, 2017, **9**, 12993–13008.
68 G. X. Yang, D. Yang, P. P. Yang, R. C. Lv, C. X. Li, C. N. Zhong, F. He, S. L. Gai and J. Lin, *Chem. Mater.*, 2015, **27**, 7957–7968.
69 L. L. Feng, D. Yang, F. He, S. L. Gai, C. X. Li, Y. L. Dai and P. P. Yang, *Adv. Healthcare Mater.*, 2017, **6**, 1700502.
70 M. H. Chan, Y. T. Pan, I. J. Lee, C. W. Chen, Y. C. Chan, M. Hsiao, F. Wang, L. D. Sun, X. Y. Chen and R. S. Liu, *Small*, 2017, **13**, 1700038.
71 M. H. Chan, Y. T. Pan, Y. C. Chan, M. Hsiao, C. H. Chen, L. D. Sun and R. S. Liu, *Chem. Sci.*, 2018, **9**, 3141–3151.
72 Y. Li, X. M. Liu, L. Tan, Z. D. Cui, X. J. Yang, Y. F. Zheng, K. W. K. Yeung, P. K. Chu and S. L. Wu, *Adv. Funct. Mater.*, 2018, **28**, 1800299.
73 R. Weissleder, *Nat. Biotechnol.*, 2001, **19**, 316–317.
74 A. B. Ormond and H. S. Freeman, *Materials*, 2013, **6**, 817–840.
75 X. C. Zheng, X. Wang, H. Mao, W. Wu, B. R. Liu and X. Q. Jiang, *Nat. Commun.*, 2015, **6**, 13525.